Chapter 3
Finite Element Method in Machining Processes: A Review

Carlos H. Lauro, Lincoln C. Brandão, Sergio L.M. Ribeiro Filho, Robertt A.F. Valente and J. Paulo Davim

Abstract An ecological production and low cost is the target of several industries. Increasingly, the product development is critical stage to obtain a great quality and fair price. This stage will define shapes and parameters that will able to reduce wastes and improve the product. However, the expense of prototypes also should be reduced, because, in general, the prototypes are more expensive that final product. The use of finite element method (FEM) can avoid much tests that reduce number of prototypes, and consequently the project cost. In the machining processes simulation, several cutting conditions can be reproduced to define the best tool and parameters in function of analyzed forces, stress, damages and others. This paper debates the use of FEM in the machining processes, shows some researches and indicates the main attributes to develop simulation studies for conventional machining and micromachining.

C.H. Lauro (✉) · R.A.F. Valente · J. Paulo Davim
Department of Mechanical Engineering, University of Aveiro, Campus Santiago, 3810-193 Aveiro, Portugal
e-mail: carlos.lauro@ua.pt

R.A.F. Valente
e-mail: robertt@ua.pt

J. Paulo Davim
e-mail: pdavim@ua.pt

L.C. Brandão · S.L.M. Ribeiro Filho
Department of Mechanical Engineering, Federal University of São João del-Rei, Praça Frei Orlando 170, Centro, São João del-Rei 36307-352, Brazil
e-mail: lincoln@ufsj.edu.br

S.L.M. Ribeiro Filho
e-mail: sergiolmrf@gmail.com

J.P. Davim (ed.), *Modern Manufacturing Engineering*, Materials Forming, Machining and Tribology, DOI 10.1007/978-3-319-20152-8_3

3.1 Introduction

The development of products with highest quality and lower cost are goals of many industries. New techniques to inspect and control the products are employed attempting to achieve these goals. However, the first step to reach these goals should happen still in the project conception. The materials, machines, tools, workers and others factors should be tightly defined, qualified and quantified avoiding damages, rework and wastes. Thus, the usage of computer means to concept the best shapes, material, manufacture process and others is commonly used in the industries as well as academic research, sport competition and others.

Engineering enables to find several softwares with this purpose. There are CAD's software that allow optimize the amount of material and check the interferences of components. However, among the computer mean applied in the mechanical engineering, the numerical simulation is the most widely applied to obtain specific characteristic in the components or devices. This technique is used to define dimensions, shapes, material and others variables on the single component (such as shaft, nut, bolt and others) or in complex equipment (such as aircraft, space shuttles, F1 cars and others).

The finite element method (FEM) is a numerical simulation technique, which when used presents an advantage of decreasing the number of produced prototypes. This technique allows eliminating prototypes that would be produced to analyze phenomena resultant of several manufacture processes and their respective parameters to chosen the better conditions. Liu and Zheng [1], used the 2D analysis in their investigation about composite used in vessels for hydrogen storage (aluminium liner and carbon fibre/epoxy composite layers). After simulation, they used a high-pressure pump to fill the vessels and observed the finite element results were in good agreement with the experimental values. In their investigation, Silva et al. [2] have used the FEM to evaluate the effect of the elastic properties variation on auxetics geometries. They studied eight geometries using FEM to select the two extremes conditions to validation.

According to Özel and Altan [3], FEM is developed for large deformation processes, such as metal cutting process that has been considered as a deformation process where the deformation is highly concentrated in a small zone. It is used to predict chip flow, cutting forces and especially the temperatures in the tool and the cutting stress during various machining conditions.

Thus, the FEM can be advantageous in the machining processes. The FEM helps to define parameter that can increase the tool life, improve the residual stresses and others. The objective of this section is to present the usage of the FEM in machining processes studies. Furthermore, this section indicates the attributes and modelling that are important to obtain great results of machining processes simulations.

3.2 Finite Element Method in Machining

A simple engineering problem involves several variables (sometime ignored or not observed) that complicate the reproduction of responses. Thus, the repeating same event will not result in obtaining the same measured values, which rarely will occurs. According to Fish and Belytschko [4], engineering phenomenon can be represented by partial differential equations, although these equations can be very difficult to solve by analytical methods.

The solution is by creating a numeric technique that is based on the study of Richard Courant, in 1943, who used triangular elements with variational principles to solve vibration problems, which some investigators claim to be the discovered this technical. In the 1950s, this technique was employed in the aerospace industry (Boeing, Bell Aerospace and Rolls Royce). In the 1960s, this technic was called "Finite Element" and E. Wilson developed one of the first finite element programs, limited to two-dimensional stress analysis that was widely used [4].

Shaw [5] affirmed that it was not viable until digital computers and suitable software became available in the 1960s due to the simultaneous solution of a large number of equations. According to Childs et al. [6], the studies applying FEM in chip formation began with Zienkiewicz and with Kakino, both in 1971, that simulated the loading of a tool against a pre-formed chip. However, it presented a number of limitations, such as disregard of the friction between the chip and tool, strain rate, temperature, the variations of materialflow stress and its purposed the shape of the chip. These limitations were removed in 1976 by Shirakashi and Usui that included chip/tool friction conditions, the temperature and material flow stress variations with strain, strain rate and temperature, thus it was possible to keep computational advantages in the simulation during chip formation and the influence of tool. In the 1980s, arose the first non-steady chip formation analysis and following the development of a chip formation with a first contact between the cutting edge and the work piece, similar to real conditions. In the 1990s, the non-steady analysis from transient to discontinuous chip formation and the first three-dimensional analysis and the introduction of adaptive meshing techniques particularly to cope with flow around the cutting edge of a tool was developed.

The FEM is a suitable alternative to reduce the long time and high cost in machining experimental. Furthermore, the experimental tests are valid alone in the condition tested and they depend on the precision of the equipment used [7]. Arrazola et al. [8] emphasize the need for continued fundamental modelling efforts. They affirmed that the prediction models have continued to make significant progress, but its end goal is to predict industry-relevant outcomes to improve the productivity. These models include cutting parameters (tool geometry, workpiece and tool materials) to calculate intermediary fundamental physical variables and obtain machining performance outcomes, such as tool life modelling. However, while input variables appear to remain unchanged, process outcomes can still change drastically.

Table 3.1 Some machining researches using finite element method

Researcher	Software	Process	Material
Zanger and Schulze [14]	Abaqus™	Turning	Ti-6Al-4V titanium alloy
Dandekar et al. [15]	AdvantEdge™	Turning	Ti-6Al-4V titanium alloy
Muhammad et al. [16]	MSC-MARC™	Turning	Ti15V3Cr3Al3Sn titanium alloy
Maranhão and Davim [17]	AdvantEdge™	Turning	AISI 316
Amini et al. [13]	MSC-MARC™	Turning	Inconel 738
	ANSYS™		7075 aluminium alloy, AISI 1045
John et al. [18]	DEFORM™	Turning	AISI 1020
Lauro et al. [19]	ANSYS™	Drilling	AISI H13
Isbilir and Ghassemieh [20]	Abaqus™	Drilling	Ti-6Al-4V titanium alloy
Schulze et al. [21]	Abaqus™	Broaching	SAE 5120

The cutting metal process simulation is a useful technique to extend the tool life prevising the temperature and stress in the tool [9]. Elbestawi et al. [10] also affirmed the usage of the FEM to understand the tool wear. Stenberg and Proudian [11] studied the residual stresses in the turning using 2D simulations because the simulations are relatively lower in calculation cost and it is fastest than 3D simulations.

Different packages have different capabilities and it is critical to select the package with the appropriate feature set to perform type of analysis with quality of the results. The results are influenced by the assumptions and solver techniques used in the package [12]. Amini et al. [13] used two different packages software in their investigation. A package was employed to analyze the process where the tool is considered to vibrate with an ultrasonic frequency and other package to model the horn and cutting tool. In the literature, it is possible to find many publications that report a various machining process simulation using different softwares, dimensions and others aspects, see Table 3.1.

Machining simulation has the advantage to predict thermal and mechanical behaviour of both material and tool, without spending time and money with experimental procedures that can improve productivity and reduced costs. However, it requires a great understanding of how the input data affect the prediction. The reason is that the reliability in the machining simulation is ensured by accuracy of the input values [22]. The input parameters cover the mechanical and the thermal properties of the workpiece, the cutting tool geometry, cutting speed, mesh definition and other, [23]. Astakhov and Outeiro [7] affirmed that the usage of FEM in process of chip removal presents several difficulties, mainly the high processing time, but it can result in a reliability of 95 %.

Ali et al. [24] analyzed the research review that used several software on the machining simulation of Ti-6Al-4V titanium alloy. They observed that machining process of Ti-6Al-4V titanium alloy is in agreement with the simulation values of

FEM. According to the authors, the accuracy based on the most of researchers between the experimental data and simulation showed results with more than 90 %.

John et al. [18] applied the FEM to study the effect on the surface roughness of the AISI 1020 using single-point tool (HSS) and insert tool (CNMA WC). They compared the FEM results with experimental tests, analyzing the influence of feed rate [deviation between 7.5 and 18.9 % (HSS) and 1.46 and 8.3 % (CNMA WC)], depth of cut [deviation between 3.74 and 18.5 % (HSS) and 2.9 and 4.9 % (CNMA WC)], cutting speed [deviation between 1.5 and 11.8 % (HSS) and 2.9 and 4.9 % (CNMA WC)] and tool geometry.

The comparison between FEM and experimental results in the turning of AISI 316 study, Maranhão and Davim [17] observed a difference in the cutting force (7.0, 12.6 and 8.9 %), feed force (15.4, 13.5 and 13.5 %), cutting power (2.5, 13.2 and 10.1 %), maximum cutting temperature (19.6, 24.4 and 24.6 %) and plastic strain (15.0, 19.9 and 1.3 %) when the feed rate was varied (0.05, 0.1 and 0.2 mm/rev).

However, the FEM has most relevant criticisms involve materialcharacterization (strain, strain rate, material hardness and temperature) and machining data (friction data at the tool–workpiece interface, chip formation and heat transfer conditions) that influence the effectiveness of the results [25]. Doman et al. [26] researched in the literature the usage of FEM in the grinding process to model approaches at the macro- and micro-scales. They found models still based on the modelling approach that is thermal structural with triangular heat flux, normal pressure and tangential stress inputs. The effect of coolant by convection cooling boundary conditions and constitutive material model employed was the thermo-elastoplastic type. However, they sustain the experimental tests to validate the results, because without broader validation these results and their applicability may be limited.

3.2.1 FEM Types

According to Özel and Zeren [27], the types of analyses in the FEM modelling of deformation processes can be described as Eulerian analysis, it is fixed in space, and Lagrangian analysis, the computational grid deforms with the material.

Benson and Okazawa [28] affirmed that Eulerian analysis is effective for the machining calculations, except the simplest formulations, because its mesh is fixed in space, eliminating the element distortion problems that can generate new free surfaces without a special algorithm. Furthermore, this analysis avoids a special algorithm because it can generate new free surfaces naturally. However, the problem proved not to be a sensitive benchmark calculation for evaluating the accuracy of the contact methods.

Carroll and Strenkowski [29] cited that the mainly advantages are that no explicit material failure criterion is required and that the elements cannot become overly distorted. This approach requires boundaries of the chip-free surface known in advance or adjusted interactively during the simulation and it eliminates the lengthy

transition to steady-state cutting and the need for an explicit material failure or separation criterion. However, an obvious drawback of neglecting workpiece's elasticity is that residual stresses cannot be predicted with the model. The model based on an Eulerian reference frame was developed which mesh with good elements that was defined in a control volume through which the workpiece material flowed.

The Lagrangian analysis embeds a computational mesh in the material domain and solves the position of the mesh at discrete points in time, which is relied by majority numerical models. This requires a criterion for the separation of the undeformed chip from the workpiece using several chip separation criteria. Lagrangian analysis can be utilized in the implicit technique (more applicable to solving linear static problems) and the explicit time method (more suitable for non-linear dynamic problems) [27].

The usage of implicit methods could be found in few studies in the literature. In the implicit integration, the global/structural matrices have to be formulated and inverted integration; and the whole system of differential equations has to be solved simultaneously. Besides, the implicit integration is unconditionally stable and the only limitation on Δt is the convergence of the solution, which is based on a predefined criterion [30].

Bäker et al. [31] decided to use an implicit method because it has a better scaling behaviour when local mesh refinement is needed. This method allows a greater range of flexible user-defined subroutines to be introduced in the simulation, with routines that can be used to implement complicated material separation criteria. Mamalis et al. [32] used the implicit method to model the precision hard cutting of AISI 52100 using the PcBN tool to analyze the cutting forces and temperatures.

In explicit method, a system of de-coupled differential equations is solved based on element-by-element basis, thus, only the elements' stiffness and mass matrices need to be formulated and inverted. The only concern is its conditional stability and the need to use very small Δt [32]. According to Coelho et al. [33], the explicit method is more suitable for events with large non-linear deformations at high strain rates and temperatures with complex contacts between surfaces, conditions typically expected in chip formation.

The application of Lagrangian or Eulerian analysis presents shortcomings, but a technique has been developed combining the best features of both analyses that succeed to a certain extent. It is known as the Arbitrary Lagrangian-Eulerian (ALE). Although this method is embedded in the finite element analysis software, it is very necessary to master the technique details, mainly to algorithms of mesh rebuilding and element variables remapping are affected by many factors [34].

Özel and Zeren [27] utilized the explicit dynamic ALE method with adaptive meshing capability and developed a simulation model for the orthogonal cutting of AISI 4340 that presented results in better predictions for machining-induced stresses, without re-meshing and without using a chip separation criterion.

3.3 Material and Tool Modelling

To obtain great results using FEM, it is necessary to assign material the desired properties using higher accuracy values. Simoneau et al. [35] affirmed that material properties used for metal cutting should be determined under situations involving large strains, high strain rates and elevated temperatures.

According to Buchkremer et al. [36], the material models can be categorized into two groups, the interaction between damage and plasticity. The machining simulations can be applied to one of several of constitutive equations to describe the material behaviour. It is essential to implement a plasticity model that describes the thermo-mechanical conditions under which the material deforms plastically, whose quality of the majority of proposed sub-models depends on the accuracy of the applied material model.

3.3.1 Johnson–Cook Model

In the FEM models of cutting an essential and desired attribute, the material model should satisfactorily represent elastic, plastic and thermo-mechanical behaviour. Based on this, the deformations on work material were observed and highlighted have great importance in the accurate flow stress models to represent work material constitutive behaviour under high strain rate deformation conditions [27]. The authors used a Johnson–Cook (J–C) model, Eq. 3.1, to define the flow stress in the machining of AISI 4340 steel in annealed condition simulation. One of first usage of this model was published by Johnson and Cook [37]. They develop a cumulative-damage fracture model to determine the characteristics of OFHC copper, Armco iron and 4340 steel, which was observed a very dependent trend on the state of hydrostatic pressure, and less dependent on the strain rate and temperature.

$$\overline{\sigma} = \underbrace{[A + B \cdot \varepsilon^{n}]}_{\text{Elasto-Plastic term}} \cdot \underbrace{\left[1 + C \cdot \ln\left(\frac{\dot{\varepsilon}}{\dot{\varepsilon}_0}\right)\right]}_{\text{Viscosity term}} \cdot \underbrace{\left[1 - \left(\frac{T - T_{\text{room}}}{T_{\text{melt}} - T_{\text{room}}}\right)^{m}\right]}_{\text{Thermal softening term}} \tag{3.1}$$

where

$A \leftrightarrow$ yield stress of the material under reference deformation conditions (MPa)
$B \leftrightarrow$ strain hardening constant (MPa)
$n \leftrightarrow$ strain hardening coefficient
$C \leftrightarrow$ strain rate strengthening coefficient
$m \leftrightarrow$ thermal softening coefficient
$T \leftrightarrow$ deformation temperature
$T_{\text{room}} \leftrightarrow$ room temperature
$T_{\text{melt}} \leftrightarrow$ melting temperature of the material

$\dot{\varepsilon}_0 \leftrightarrow$ reference strain rate (1/s)
$\dot{\varepsilon} \leftrightarrow$ equivalent plastic strain normalized with a reference strain rate
$\varepsilon \leftrightarrow$ plastic equivalent strain

According to Dandekar and Shin [38], the Johnson–Cook model, that has been used in many studies, is based on experimentally determined flow stresses as a function of strain, temperature and strain rate in separate multiplicative terms. Sartkulvanich et al. [39] present two equations that were modified from J–C model. The first modified model takes the blue brittleness effect in low carbon steel into account, Eq. 3.2, and the second model is used for materials that do not exhibit blue brittleness, Eq. 3.3. The authors affirmed that these models assume to have no effect of coupling and reduce the problem of non-uniqueness. Furthermore, a small number of parameters are preferred for reducing computational time and promoting computational robustness. The parameter '*A*' is disregarded due to no initial stress assumption used in Oxley's theory.

$$\overline{\sigma} = B \cdot \varepsilon^n \cdot \left[1 + C \cdot \ln\left(\frac{\dot{\varepsilon}}{\dot{\varepsilon}_0}\right)\right] \cdot \left[\left(\frac{T - T_{\text{room}}}{T_{\text{melt}} - T_{\text{room}}}\right) + a \cdot \mathrm{e}^{-0.00005 \cdot (T-700)^2}\right] \tag{3.2}$$

$$\overline{\sigma} = B \cdot \varepsilon^n \cdot \left[1 + C \cdot \ln\left(\frac{\dot{\varepsilon}}{\dot{\varepsilon}_0}\right)\right] \cdot \left[1 - \left(\frac{T - T_{\text{room}}}{T_{\text{melt}} - T_{\text{room}}}\right)^m\right] \tag{3.3}$$

Besides usage of elastic, plastic and thermo-mechanical behaviour modelling, it is necessary to assign a damage model. Chen et al. [40] used an energy-based ductile failure criterion to simulate HSM of Ti-6Al-4V titanium alloy. According to Ambati and Yuan [41], the damage modelling in orthogonal cutting has significant importance because the most part of the failure occurs due to thermal softening and to form the chip. It should be detached from the workpiece material to which fracture criterion should be applied. The Johnson–Cook damage criterion, Eq. 3.4, is found in the literature used by several researches. Duan and Zhang [42] cited that the damage parameters can be uniquely determined independent of the cutting conditions and its usage as criterion for chip separation in HSM can avoid the problems in the simulations using other criteria.

$$\bar{\varepsilon}_{\text{f}} = \left[D_1 + D_2 \cdot \mathrm{e}^{\left(D_3 \cdot \frac{p}{\sigma_e}\right)}\right] \cdot \left[1 + D_4 \cdot \ln\left(\frac{\dot{\varepsilon}^{\text{p}}}{\dot{\varepsilon}^0}\right)\right] \cdot \left[1 + D_5 \cdot \left(\frac{T - T_{\text{room}}}{T_{\text{Melt}} - T_{\text{room}}}\right)\right] \tag{3.4}$$

where

$D_1 \leftrightarrow$ Initial failure strain
$D_2 \leftrightarrow$ Exponential factor
$D_3 \leftrightarrow$ Triaxiality factor
$D_4 \leftrightarrow$ Strain rate factor
$D_5 \leftrightarrow$ Temperature factor

$T \leftrightarrow$ deformation temperature
$T_{room} \leftrightarrow$ room temperature
$T_{melt} \leftrightarrow$ melting temperature of the material
$\bar{\varepsilon}_f \leftrightarrow$ failure plastic strain for damage initiation
$\dot{\varepsilon}^p \leftrightarrow$ equivalent plastic strain rate
$\dot{\varepsilon}^0 \leftrightarrow$ plastic strain rate
$\frac{p}{\sigma_e} \leftrightarrow$ ratio between hydrostatic pressure to equivalent stress

Shrot and Bäker [43] proposed a method for inverse determination of J–C constants using the chip morphology and the cutting force encountered during the high-speed cutting process. They found an optimal parameter set returned by the simulation produces results which are indistinguishable from the results produced by the original set, although it is possible to re-identify J–C parameters by inverse methods and the existence of noise in the error function poses a hurdle in re-identifying the original J–C constants.

Umbrello et al. [44] investigated the influence of the constants used in the J–C model on the forces, temperatures, chip morphology and residual stresses in the machined components of AISI 316L steel, comparing with experimental data. They applied five different sets where two sets were used with high strain rate mechanical. The tests were carried out on hat-shaped specimens applying the Split Hopkinson's Pressure Bar (SHPB) method. Moreover, instrumented orthogonal milling tests were carried out to generate information about material flow stress in machining based on different analytical chip formation models. One set identified using SHPB tests that were carried on cylindrical compression specimens. One set based on SHPB experiments using hat-shaped specimens and the last one set determined using a methodology based on analytical modelling of the orthogonal cutting process along with metal cutting experiments.

Yan et al. [45] studied an approach to characterize the stress response of workpiece in hard machining of AISI H13 die steel (30–60 HR_C). They presented a methodology expressed by coupling the reference flow stress curve at the certain workpiece hardness that taken an advantage of the form of the Johnson–Cook model, incorporating strain, strain rate and thermal softening effects. This isotropic thermal-elastic-plastic model, which considers the influence of the workpiece hardness on the flow stresses, is showed by the Eq. 3.5.

$$\overline{\sigma} = [A + B \cdot \varepsilon^n + C \cdot \ln(\varepsilon_0 + \varepsilon) + D] \cdot \left[\left(1 + E \cdot \ln\left(\frac{\dot{\varepsilon}}{\dot{\varepsilon}_0} \right) \right) - \left(1 - \left(\frac{T - T_{room}}{T_{melt} - T_{room}} \right)^m \right) \right] \tag{3.5}$$

where the C and D are the function of the initial workpiece hardness accounted for the influence of hardness, which are determined by Eqs. 3.6 and 3.7, respectively. The E is the strain rate strengthening coefficient (C in the Eq. 3.1).The ε_0 is the reference strain and is taken to be 10^{-3}. The other variables are described in the Eq. 3.1.

$$C = 0.0576 \cdot (\mathrm{HR}_C)^2 - 3.7861 \cdot (\mathrm{HR}_C) + 52.82\,(\mathrm{MPa}) \tag{3.6}$$

$$D = 0.6311 \cdot (\mathrm{HR}_C)^2 - 12.752 \cdot (\mathrm{HR}_C) - 727.5\,(\mathrm{MPa}) \tag{3.7}$$

3.3.2 Zerilli–Armstrong Model

The Zerilli–Armstrong (Z–A) model was developed for relatively simple materials where the dislocation slip in several kind of crystal structures was considered. This formulation considers slip based on dislocation physics, which can describe the flow stress as appropriate for the Johnson–Cook model. The Z–A not take into account the damage induced by secondary phase particles due to be a failure mechanism based solely on the constitutive law. The comparison between the Z–A and J–C models for the AISI D2 steel and observed that the Z–A showed a more accurate estimate for higher temperature range and is less accurate for low temperatures [46].

According to Liu et al. [47], the Z–A model is derived from the thermal activation theory of dislocations and widely used for analyzing the dynamic response of metals over a range of temperatures and strain rates. The authors affirmed that there are two physical sources of flow softening at high strains. The first is due to the materialfailure in the shear band because of the void and crack formation, which depends on both strain and the strain rate. The second is due to the dynamic recovery, which causes flow softening at high strains and is captured by the square root term in the Z–A model.

Moćko and Kowalewski [48] cited that Z–A model compared to J–C model is that reflects the coupled influence for both temperature/strain and strain rate/temperature on the mechanical characteristics. In the X4CrMnN16-12 austenitic steel modelling, they observed that the Z–A model gave the worst results related to a phase transformation during plastic deformation process.

Zerilli and Armstrong [49] presents a description of stress components that combine to determine the plastic flow stresses showing two separate reasonably explicit expressions for their constitutive behaviour. One is for the body-centred cubic material (bcc), where the temperature softening and strain-rate hardening depends on "*u*" and are higher with the increase of strain hardening, as can be seen in Eq. (3.8). The other is face-centred cubic (fcc), which exhibits dependencies uncoupled of the strain hardening factor from the strain-rate hardening, thermal softening and the grain size, according to Eq. (3.9). The authors also showed a model where the thermal activation stress and the effect of yield stress on grain size are considered due to the requirement of slip band-stress concentrations at grain boundaries being needed for the transmission of plastic flow between the polycrystal grains.

$$\sigma_{\text{th}} = C_1 \cdot \mathrm{e}^{-C_3 \cdot T + C_4 \cdot T \cdot \ln \dot{\varepsilon}} \tag{3.8}$$

$$\sigma_{\text{th}} = C_2 \cdot \varepsilon^{1/2} \cdot \mathrm{e}^{-C_3 \cdot T + C_4 \cdot T \cdot \ln \dot{\varepsilon}} \tag{3.9}$$

where

$\sigma_{\text{th}} \leftrightarrow$ thermal component of the shear stress
C_1, C_2, C_3 and $C_4 \leftrightarrow$ undetermined coefficients
$T \leftrightarrow$ current temperature minus reference temperatures
$\dot{\varepsilon} \leftrightarrow$ being the strain rate

3.3.3 Others Models

Buchkremer et al. [36] presented in their paper the modified Bai-Wierzbicki (MBW) material model to simulate the longitudinal turning processes with steel AISI 1045. The MBW model integrates a damage variable into the yield potential for the description of material degradation. The MBW model shows great potential to predict the softening behaviour of the material and the damage approach enables the prediction of possible failure behaviours like serrated chip formation or chip breakage. Furthermore, it is further extended with the consideration of temperature and strain rate effects, whose influences are significant in machining. The validation tests showed that the chip formation, cutting temperatures, and mainly, the cutting forces were in close agreement with each other.

Besides J–C and Z–A models, the Rusinek and Klepaczko (RK) model, Eq. (3.10) can be much more precise description of the mechanical properties variation of materials, in question, particularly under dynamic loads. This model decomposes the equivalent stress into internal stress, effective stress and viscous-drag stress. In addition, the model considers the effective stress and it presented coupled relationships between strain rate and temperature. The use of the RK model showed best results [48].

$$\bar{\sigma}\left(\bar{\varepsilon}_p, \dot{\bar{\varepsilon}}_p, T\right) = \frac{E(T)}{E_0}\left[\sigma_\mu\left(\bar{\varepsilon}_p, \dot{\bar{\varepsilon}}_p, T\right) + \sigma^*\left(\dot{\bar{\varepsilon}}_p, T\right)\right] + \bar{\sigma}_{vs}\left(\dot{\bar{\varepsilon}}_p\right) \tag{3.10}$$

where

$\bar{\sigma}\left(\bar{\varepsilon}_p, \dot{\bar{\varepsilon}}_p, T\right) \leftrightarrow$ overall flow stress
$\sigma_\mu\left(\bar{\varepsilon}_p, \dot{\bar{\varepsilon}}_p, T\right) \leftrightarrow$ internal stress component
$\sigma^*\left(\dot{\bar{\varepsilon}}_p, T\right) \leftrightarrow$ effective stress component
$\bar{\sigma}_{vs}\left(\dot{\bar{\varepsilon}}_p\right) \leftrightarrow$ drag stress component
$E(T) \leftrightarrow$ temperature dependence of the Young's modulus
$E_0 \leftrightarrow$ Young's modulus at $T = 0$ K,
$T \leftrightarrow$ temperature
$\dot{\bar{\varepsilon}}_p \leftrightarrow$ strain rate
$\bar{\varepsilon}_p \leftrightarrow$ inelastic strain

3.3.4 Tool

Generally, the tools are not applied in complex model to characterize the material. In some studies, the tool material is defined by thermal and/or mechanical proprieties. Tang et al. [50] considered the thermal (thermal conductivity, thermal expansion, specific heat capacity) and mechanical properties (Young's modulus, Poisson's ratio, density, tensile strength) proprieties to cBN tool. Fathipour, Hamedi and Yousefi [51] used only density and Young's modulus to characterize the tool. Santiuste et al. [52], Shrot and Bäker [43], Manikandan et al. [53] considered the tool as rigid body, which is not applied to the proprieties. Based on this, the results obtained by these preliminary studies show that more researches about tool modelling should be developed to complete the total understanding about machining process using finite element methods.

3.4 Meshing and Re-meshing

The definition of meshing requires great caution, because of the element type and element size interference in the results and also due to computational effort. Ambati and Yuan [41] emphasized that numerical simulations are verified with measured cutting force that is insensitive to the element size. In their work, they studied the chip formation from computational simulation analyzing the effect of element size that leads to a direct modification in failure criterion. They observed that the finite element size changes chip morphology significantly and a failure model can transform the chip from continuous to segment. Furthermore, the dependence on element size can be eliminated by a simple non-local damage model based on characteristic element length, generating a unique solution of cutting chip if the temperature can be neglected.

To model the turning process of Ti-6Al-4V titanium alloy, Dandekar et al. [15] used an updated-Lagrangian FEM along with continuous re-meshing. They adopted tetrahedral finite elements, 4-node and 12 degree of freedom and the minimum element edge length for the chip bulk of 0.0198 mm, cutter edge of 0.01 mm and the radius of refined region was set as 0.075 mm. Santiuste et al. [52] used a medium element size at this zone, and this size was 5 μm in the orthogonal cutting of glass and carbon fibre composites developed with plane stress, quadrilateral, linearly interpolated, elements, with reduced integration and automatic hourglass control.

Shrot and Bäker [43] used a plane strain elements with 4-node bilinear and reduced integration applying the hourglass control to simulate orthogonal cutting of AISI 52100. Zanger and Schulze [14] defined the coupled temperature-displacement using plane strain elements with 4-node bilinear displacement and temperature to simulate the cutting of Ti-6Al-4V titanium alloy. Seshadri et al. [54] modelled the workpiece (6 mm × 2 mm) using of iso-parametric quadrilateral element type with size of 0.057 mm, 4,680 nodes and 4,500 elements.

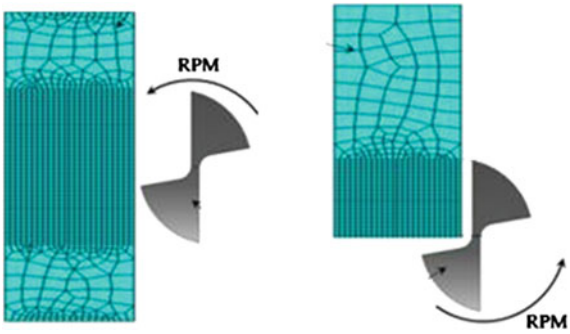

Fig. 3.1 Example of workpiece meshing (Adapted from [56], with permission from Springer)

According to Bäker et al. [31], the simulation has to meet the following requirements as usage of quadrilateral elements (as regular as possible, avoiding extremely distorted meshes); high mesh density in the shear zone; discontinuous deformation (segmentation) of the chip; convergence of the implicit algorithm; and usage of standard software for portability and flexibility.

It is known that a refined meshing will improve the results, but it will need high investments in computer and time. Many researchers use the deformation section a meshing more refined than the workpiece rest, it decrease the elements number and the simulation time, Fig. 3.1. Kouadri et al. [55] defined a coupled displacement–temperature four nodes element with minimum element, sized about 10 μm, in the chip zone that was chosen after mesh convergence tests and a compromise between result accuracy and reasonable CPU time.

The cutting simulation presents an additional degree of complexity due to need of a proper modelling of both large plastic deformations. This should be considered from the mathematical point of view and because it cause rapid solution degradation due to element distortion and material removal. In spite of a problem be tackled using pre-distorted meshes, this technique was essential to obtain reliable numerical solutions, thus it was adapted of adaptive re-meshing techniques, which encompass three main aspects: Meshing techniques, Error and distortion metrics guiding the re-meshing, and Data transfer from old to new mesh [57]. Schulze et al. [58] considered the high mesh deformations in the material separation zone to simulate the broaching process, however, as example, it can be commented that the separation of the material lead to a loss of information due to the deletion of element or nodes.

Saffar et al. [59] affirmed that the meshing nodes are moved to more favourable positions to improve mesh distortion. The solution-dependent meshing is supplied to concentrate mesh towards with the developing boundary concave, aiming the chip separation area approximately in the cutting edge with generating local mesh refinement in this area. Furthermore, the authors cited that the mesh is adaptively designed to create a new spatial discrimination and the mesh quality is improved: *h*-adaptively, *p*-adaptively and *r*-adaptively.

According to Vaz et al. [57], the *h*-adaptivity consists of changing the element size *h* that can be used to generate well-shaped elements. The new mesh has a

Table 3.2 Comparison of re-meshing methods [57]

Methods	Advantages	Disadvantages
General *h*-method	The most general and flexible method	Requires more elaborate algorithms
Hierarchical *h*-method	Fast method. Easy to implement for regular mesh	Difficult to implement for irregular mesh. Will not reduce element distortion
r-Method	Easy to implement. Inexpensive	Limited capacity to improve mesh
p-Method	Fast and simple	The degree in the shape functions cannot be increased too much so the improvement is limited. Cannot reduce element distortion

different number of elements and the connectivity of the nodes is changed. The authors also highlighted the hierarchical *h*-method, which is a hierarchy between old and new elements and the approach. The *r*-adaptivity consists of relocation of the nodes without changing the mesh connectivity, which is called smoothing when used to improve the shape of elements. In the *p*-adaptivity, the degree of the interpolating polynomials is changed in order to increase the accuracy of the solution. A comparison of these methods is presented in the Table 3.2.

3.5 Boundary Conditions

The boundary conditions can be defined in two types, the first was a mechanical condition applied on the bottom face of the workpiece fixed in the feed and cutting directions. The second showed a condition where the cutting speed is applied to the rigid tool and a thermal condition with initial configuration an initial temperature that considered the workpiece–tool couple. Both conditions were considered during the chip formation at the tool–workpiece contact zone [55]. These authors also neglected heat exchange with the environment to obtain a significant heat exchange with environment that can influence the chip formation process due to the simulated cutting duration is very short, few microseconds.

Vaz et al. [57] highlighted the great importance of contact due to the important effects associated with the tool–chip interface, which is commonly solved by penalty approach, such as method of Lagrangian multipliers or a combination of penalty and Lagrangian multiplier methods. The latter is as in the augmented Lagrangian technique, with the aim of retaining the merits of each approach. Saffar et al. [59] highlighted the high stresses, high strain rates and high temperatures can cause a high mechanical power which is dissipated in the tool–chip interface leading to many structural modifications of the contacting pieces. Thus, there is no law for universal contact which can predict friction forces among a wide range of cutting conditions.

In their study of the cutting modelling, Malakizadi et al. [60] assumed that the workpiece material was a rigid-perfectly plastic. The tool was considered a rigid

body, where the heat transfer within the tool was allowed. Beyond the heat transfer coefficient between the tool and chip interface was assumed to be 10^5 N/s•mm•C to ensure that the heat transfer reaches steady-state condition at the end of the simulations.

3.5.1 Chip Separation

Saffar et al. [59] affirmed that the chip formation occurs due to chip separation (geometrical and physical) criterion and model realization. The geometry of chip separation occurs when the distance between the nearest workpiece's node on the moving path of the cutting edge and the cutting edge is equal to or smaller than this given distance value. For the physical criteria, the magnitude of distribution of shear stress, effective stress or effective plastic strain has a major effect on mesh distortion together with the value of maximum shear stress, and the effective stress in the machined surface. According these authors, the model realization is related to the software applied and there are several methods in a finite element mesh, as:

- Element removal: when the physical criterion is reached, the material failure happens and the element carries no stress any more as if it does not exist. Such elements can be removed and will not be displayed.
- Node debond: the chip and the workpiece are two separated parts. They are perfectly bonded together through some pair of nodes along the prospective parting line.
- Node splitting: the front of cutting edge separates the element and creates new nodes at this region. Through the further movement of the cutting tool, the two elements move in different directions and lose contact.
- Mesh adaptively: Chip separation is performed by mesh refinement in the separation zone by increasing the number of elements or relocation of the nodes.

For Vaz et al. [57], the chip formation can be reproduced in continuous, discontinuous and intermediate forms that follow three basic strategies: continuous chip separation along a pre-defined cutting plane; chip separation and breakage; no chip separation. They mentioned that most common approach predefines a chip separation line (or plane), along which a separation indicator is computed. Also, they highlighted several chip separation as Nodal distance, Equivalent plastic strain, Energy density, Tensile plastic work, Stress index, Maximum principal stress, Johnson–Cook, Damage considerations and others.

Özel and Zeren [27] affirmed that the FEM models should not require chip separation criteria that highly deteriorate the physical process simulation around the tool cutting edge, especially in the presence of dominant tool edge geometry. Duan and Zhang [42] suggest the use of Johnson–Cook models for chip separation and the modified Zorev model for tool-chip friction description to predict precisely the serrated chip formation and cutting force in HSM.

In their paper, Chen et al. [40] analyzed the variations of chip morphology with cutting speeds and feed rates in the HSM of Ti-6Al-4V titanium alloy, which observed that the dimensions of segment chip morphology increase with feed rate and the degree of segmentation is more obvious under higher cutting speeds. Pu et al. [61] used the chip morphology to calibre their numeric tests that showed a differences range from 10 to 20 % to the experimental results.

3.6 Friction

Besides the material characterization, another aspect that is important in the cutting simulation is determining the friction coefficient. According to Isbilir and Ghassemieh [20], the contact and the friction parameters between the tool and workpiece are influenced by the cutting speed, feed rate, geometry and the surface properties. Özel and Zeren [27] emphasized that the interfacial friction characteristics on the tool/chip and tool/work contacts should be modelled with high accurately in order to account for additional heat generation and stress developments due to friction.

Arrazola and Özel [62] studied the importance of detailed friction model to improve the results. They observed differences between predicted and experimental forces when comparing the forces between the Coulomb friction and the sticking-sliding friction reveals important findings. It exhibited the influence is larger over the thrust force since it decreases by 35 %, while the cutting force decreases only by 11 %. In the literature it is possible to find several models to determine the friction coefficient. The usage of the Coulomb's law is employed to determine the friction coefficient. Coulomb's law was generally used in the sliding region that is located next to the sticking region up until the point where the chip leaves the tool, Eq. (3.11). The relatively low normal stresses and small plastic deformation, friction behaviour in this region is characterized by the real area of contact. Thus, the frictional stress can be assumed to be dependent of the normal stress. The shear stress decreases from a constant value at the sticking region to zero at the location where the chip leaves from the tool rake face.

$$\tau = \mu \cdot \sigma_n \tag{3.11}$$

where

$\tau \leftrightarrow$ frictional stress

$\mu \leftrightarrow$ coefficient of friction

$\sigma_n \leftrightarrow$ normal stress

According to Isbilir and Ghassemieh [20] Coulomb friction model is used and a constant friction coefficient of 0.5 is used in the analysis. Maranhão and Davim [17] simulated the turning of AISI 316 using a cemented carbide tool with a chip breaker and coating of TiCN-Al_2O_3-TiN. They applied the Coulomb model, Eq. (3.12), to provide a first approach to the friction value (0.89, 0.80 and 0.53) and time later,

they needed several iterations must be carried until the results are satisfactory (1.1, 1.0 and 0.95). The authors justified this correction due to a change of friction coefficient is a fast and reliable way to minimize differences between experimentation and simulation. Besides, the software did not allow a change of Johnson–Cook coefficients, which could allow a disagreement between numerical and analytical results due to the critical friction coefficient.

$$\mu = \frac{F_T + F_c \cdot \tan\gamma}{F_c - F_T \cdot \tan\gamma} \tag{3.12}$$

where

$F_T \leftrightarrow$ thrust (feed) force
$F_c \leftrightarrow$ cutting force
$\gamma \leftrightarrow$ tool rake angle

Özel [63] cited that in the first simulations, the friction in the metal cutting was largely ignored or assumed to be constant based on Coulomb's law at the entire tool–chip interface. Many researchers utilized Zorev's model in simulations of orthogonal cutting. They studied the influence of implementing different friction models in the simulation for orthogonal cutting of low-carbon free-cutting steel with P20 carbide cutting tool by comparing the output variables (cutting force, thrust force, chip-tool contact length, shear angle and maximum temperature at tool–chip interface) to experimental results. These comparisons showed that the friction models had a significant influence in predicting chip geometry, forces, stresses on the tool and the temperatures at the tool–chip interface. The predictions are clearly found to be most accurate when utilizing friction models based on the measured normal and frictional stresses on the tool rake face and when implemented as variable.

According to Manikandan et al. [53], the friction condition is an important factor that influences the chip formation, cutting load and surface finish quality. They used the combination of the Coulomb's friction model and shear (sticking) friction model, Eq. (3.13).

$$\tau = \begin{cases} \mu\sigma & \tau < k \\ k & \tau \geq k \end{cases} \tag{3.13}$$

where

$\tau \leftrightarrow$ surface friction stress
$\mu \leftrightarrow$ friction coefficient
$k \leftrightarrow$ surface normal stress and shear flow stress

Duan and Zhang [42] proposed the modified Zorev's model to describe the chip-tool friction, which was used to analyze the friction influence related to the tool rake angle with an inverse relation. According to Haddag et al. [64], the contact zone a part of the heat flux q is generated by friction that can be written as the sum of inelastic work heat flux due and friction work heat flux. They applied the Eq. (3.14)

to evaluate the heat flux generated by friction at the contact interface. In the orthogonal cutting of Al 2024-T351 aluminium alloy, applying a cutting speed of 60 m/min, feed of 0.4 mm/rev and depth of cut of 0.5 mm, they assumed that the frictional work converts into heat (η_f) was 1. The fraction of the thermal energy conducted into the chip (f_f), which depends on the thermal proprieties of the tool and workpiece material as well as the temperature gradient near the chip/tool interface was 0.5.

$$\dot{q}_f = f_f \cdot n_f \cdot \tau \cdot \dot{\gamma} \tag{3.14}$$

where

$\dot{q}_f \leftrightarrow$ friction work heat flux
$f_f \leftrightarrow$ fraction of the thermal energy conducted into the chip
$\eta_f \leftrightarrow$ frictional work conversion factor
$\tau \leftrightarrow$ friction stress given by Eq. (3.10)
$\dot{\gamma} \leftrightarrow$ slip rate

Knowing that the friction is an important aspect in machining processes (experimental or modelling), especially during dry condition, Ulutan and Özel [65] developed a new methodology to determine tool friction on orthogonal cutting of Ti-6Al-4V titanium and IN-100 nickel-based alloys using uncoated tungsten carbide (WC/Co) tool. In this study, they considered unworn and worn tool geometry. They observed that the friction coefficients did not depend on most of the cutting parameters in machining titanium and nickel-based alloys and slightly with cutting edge geometry.

According to Özel and Altan [66], the friction conditions at the chip–tool contact can be interpreted in terms by shear friction and friction coefficient, Fig. 3.2. They used an appropriate initial value for the friction coefficient ($\mu_{p,\text{initial}}$) selecting as the ratio of the frictional force (F_f) and normal force (F_n) acting on the tool rake face that were calculated from the measured force components at the given rake angle.

Malakizadi et al. [60] developed a subroutine to include pressure dependencies on shear friction model at chip/tool interface using the Eq. (3.15). They affirmed

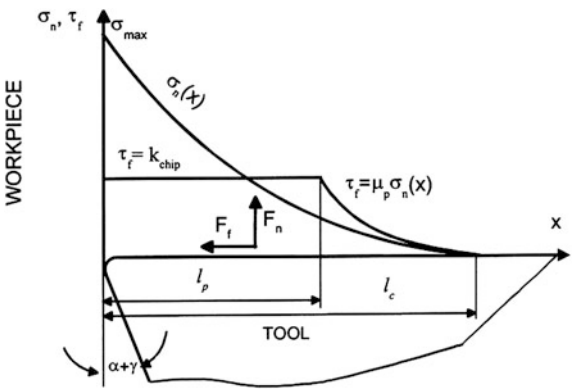

Fig. 3.2 The normal and frictional stress distributions (Adapted from [66], with permission from Elsevier)

that, for the aluminium alloy and Grey Cast Iron, the constants of the model, α (0.012 and 0.0035) and m_0 (1), were kept constant.

$$\tau = m_0 \cdot [1 - \exp(\alpha \cdot P)] \cdot k \tag{3.15}$$

where

$\tau \leftrightarrow$ frictional shear stress
$K \leftrightarrow$ shear strength of the workpiece material
$P \leftrightarrow$ pressure
m_0 and $\alpha \leftrightarrow$ model constants.

Muhammad et al. [16] affirmed that the effect of friction on the tool–workpiece interface is accounted for its effect on the cutting forces. They used a modified shear friction model to adequately represent the friction behaviour at the tool–workpiece interface, Eq. (3.16).

$$\sigma_{\text{fr}} \leq -m_{\text{fr}} \cdot \frac{\bar{\sigma}}{\sqrt{3}} \cdot \frac{2}{\pi} \cdot \text{sgn}(V_{\text{r}}) \cdot \arctan\left(\frac{V_{\text{r}}}{V_{\text{cr}}}\right) \tag{3.16}$$

where

$\sigma_{\text{fr}} \leftrightarrow$ friction stress
$\bar{\sigma} \leftrightarrow$ equivalent stress
$V_{\text{r}} \leftrightarrow$ relative sliding velocity
$V_{\text{cr}} \leftrightarrow$ critical sliding velocity
$m_{\text{fr}} \leftrightarrow$ friction coefficient
sgn $(x) \leftrightarrow$ signum function of x

According to Özel [67], the constant friction models may not represent the sophisticated contact conditions that exist in the 3D engagement of the micro-geometry tool edge and the workpiece. The friction zones are also difficult to be implemented in 3D problems. According to the literature, it can be found several friction values to different machining processes types. Coelho et al. [33] cited that the FEM software used does not allow the shear stress limit to vary, therefore, the value of 329 MPa was set, using the initial equivalent stress of 950 MPa and an average friction coefficient of 0.60 and suggests to uncoated PcBN a coefficient of 0.35.

Rotella et al. [68] compared the experimental and numeric results of turning of Al 7075-T651 aluminium alloy that showed differences between the values, especially for the radial force. These differences can be justified by use of 3D FEM model that has still problem as friction models. These models were well tested in orthogonal machining, but in the 3D model have taken into account the influence of tool geometry parameters (tool nose radius, angles, etc.), as well as the grain size.

In the composite cutting, although the friction model between workpiece and tool is required, an accurate value remains an issue for several reasons [69]. To simplify the process, Mahdi and Zhang [70] ignored friction in the orthogonal cutting of the fibre-reinforced composite. Phadnis et al. [71] considered the 0.03 the friction coefficient at the interface between cutting edge and laminate in the

Table 3.3 Same values of friction coefficient using in machining researches

Researcher	Tool material	Workpiece material	vc (m/min)	Feed (μm/rev)	Depth (mm)		Friction
Turning							
Özel and Altan [66]	Uncoated carbide	AISI P20 (30 HR_C)	200, 300 and 550	51, 75, 100	1		0.5–0.7
				25			1
Seshadri et al. [54]	WC-Co/TiAlN	2024-T351 aluminium alloy	66, 102, 157	102, 205, 318	1		0.43
Kouadri et al. [55]	WC-Co	2024-T351 aluminium alloy	30–500	50, 300	4		0.2
Milling							
					ap	ae	
Saffar et al. [59]	HSS (ϕ6 mm)	AISI 1045	47.12	ago/40	4–7.5	2.5	0.32
	HSS (ϕ3 mm)		23.56	ago/50	1.5–5	1.5	
Drilling							
				f (mm/min)	Diameter		
Isbilir and Ghassemieh [20]		Ti-6Al-4V	35.2	95–171	8 mm		0.5
Broaching							
Schulze et al. [21]		SAE 5120	30, 60, 90	40 μm			0.35, 0.50

ultrasonically assisted drilling of CFRP composite. To model the drilling on CFRP composite, Phadnis et al. [72] used a coefficient of friction of 0.3. Santiuste et al. [52] assumed a constant coefficient of friction equal to 0.5 in the orthogonal cutting of glass and carbon fibre reinforced polymer composite. In the orthogonal cutting of metal matrix composite (MMC), Al 6061 aluminium alloy reinforced with silicon carbide particles, Pramanik et al. [73] employed a coefficient of friction of 0.62. The Table 3.3 shows the friction values applied in some machining researches.

3.7 Examples of Employments

The cutting metal simulation is commonly employed to predict the phenomena and events in the machining. One of reasons to this is the facility to measure machining phenomena. Arrazola and Özel [62] affirmed that it is very costly and difficult to

measure stresses and temperatures in high-speed machining using experimental tests. Umbrello et al. [44] cited that the good agreement obtained between the experimental and numerical results indicate that the proposed FEM model appears to be suitable for studying the influence of cutting parameters on residual stress. Manikandan et al. [53] used orthogonal cutting to analyze plane strain-coupled thermo-mechanical.

To understand the influence of cutting speed and feed conditions in the built-up edge (BUE) formation in machining carbon steels based, Childs [74] analyzed flow stress in the absence of failure depending of the strain, strain-rate and temperature. The modelling and simulations confirm the importance of the blue-brittle effect for BUE formation in steel machining. In the agreement between predicted and experimental BUE speed ranges it was necessary to reduce the temperature for maximum blue-brittle effect from the expected 600 to 400 °C and a need for more data on or understanding of ductile shear failure of steels in the compressive (pressure from 0 to 0.75 of flow stress) and temperature (up to 600 °C) conditions of chip formation in BUE conditions.

Buchkremer et al. [36] highlight that the cutting force is the integral representations of the calculated flow stresses in the primary shear zone, showed excellent results for a broad range of cutting conditions.

The usage of FEM to resolve machining operation is generally applied due to it involves intense thermo-mechanical phenomena. Each material point in the cutting tool and the workpiece should satisfy simultaneously the Mechanical (3.17) and Thermal (3.18) equilibrium equations that are strongly coupled, since the stress tensor (σ), in the mechanical equilibrium equation, depends on the temperature variable (T). Furthermore, a part of the mechanical inelastic work transforms to heat, so a part of the heat flux q is a function of the flow stress and the plastic strain [64].

$$\operatorname{div}\sigma + f_v = p\ddot{u} \tag{3.17}$$

where

$\sigma \leftrightarrow$ Cauchy stress tensor
$f_v \leftrightarrow$ body forces
$\ddot{u} \leftrightarrow$ acceleration

$$k\nabla^2 T - \rho \cdot c_p \cdot \dot{T} + \dot{q} = 0 \tag{3.18}$$

where

$k \leftrightarrow$ thermal conductivity
T $\leftrightarrow$ temperature
$\rho \leftrightarrow$ material density
$c_p \leftrightarrow$ thermal capacity
$q \leftrightarrow$ heat flux

Weinert and Schneider [75] affirmed that FEM has proven to be advantageous for describing the thermal and thermo-mechanical stress and can establish a direct link between the thermal stress and the application properties of the tool during grinding. The use of FEM in cutting processes are emerging as useful techniques for predicting tool temperatures and stresses and for extending tool life [9].

According to Rizzuti et al. [25], besides the 2D model, the few milliseconds of cutting time are one of the main problem in temperature modelling because there are several problems related to heat generation and diffusion into the tool. In fact, no steady-state conditions are reached during the numerical simulation.

Rotella et al. [68] studied the effects of cutting speed and tool geometry on the grain size evolution in the turning of Al 7075-T651 aluminium alloy. After the calibration to determine the frictions values (m and μ), they applied a subroutine to predict the dynamic recrystallization process by Zener–Hollomon equation and the hardness modification using the Hall–Petch equation. This proposal provided a good prediction of the microstructural alteration that was affected by cutting speed and the tool nose radius.

Pu et al. [61] used a 2D model to predict grain size in turning of AZ31B magnesium alloy on the dry and cryogenic cooling system. They developed a subroutine applying the Zener–Hollomon equation that showed a successfully predicted the grain refinement on the surface and sub-surface.

Duan et al. [76] used the FEM simulation to study the thickness of white layer based on phase transformation mechanism. They analyzed the effects of mechanical factors on transition temperature were taken into account explicitly. They observed an influence of cutting parameters on the thickness of white layer, i.e. the thickness of white layer varies significantly with the variations of cutting speed, depth of cut, flank wear and chamfer geometry of tool.

Attanasio et al. [77] used numeric (2D and 3D) and experimental tests to study the formation of layers on the orthogonal hard turning of AISI 52100. They found that the thickness of white and dark layers increases with increasing of tool flank wear and higher cutting speed generates thicker white layers and thinner dark layers. A small feed rate increases the white layers thickness; on the other hand, the high feed rate decreases the dark layer thickness.

Ramesh and Melkote [78] used the FEM to study the white layer formation in orthogonal machining of AISI 52100 (62 HR_C) using the cBN tool. They used a model explicitly incorporates the effects of stress and strain on the transformation temperature, volume expansion and transformation plasticity that showed predicted values and trends of white layer thickness. These effects are in good agreement with the measured values and trends when compared to experimental validation.

Sometime, many investigators using the FEM to study the residual stress behaviour on the machining processes. Thus, for example, Ee et al. [79] used a 2D model to study the residual stresses induced by orthogonal machining. Valiorgue et al. [80] used a 3D model to study the residual stresses in finish turning of AISI 304L stainless steel with a TiN coated carbide tool. They proposed a model that does not simulate the chip formation and the material separation around the cutting

edge, but only onto the thermo-mechanical loadings applied onto the machined surface.

Rizzuti et al. [25] affirmed that the residual stresses are generated by the material deformation and by the thermal cycle and both phenomena occur during the cutting process. The components of the residual stresses can be the axial and the circumferential. They measured the circumferential stress using the numerical procedure of orthogonal cutting of AISI 1045, which observed agreement was obtained between the numerical predicted residual stresses and those experimentally measured.

Özel and Zeren [27] used the FEM to study machining with round edge cutting tools in the HSM of AISI 4340 and they compared with experimentally measured residual stresses obtained from the literature, which indicated an influence the stress and temperature fields greatly. These predictions combined with the temperature field predictions are highly essential to further predict surface integrity and thermo-mechanical deformation related property alteration on the microstructure of the machined surfaces.

Ji et al. [81] modelled the orthogonal cutting of TC4 alloy applying MQL effects and they analyzed the heat transfer coefficient that are all considered in the residual stress prediction model. Their model gives a relationship between the flow rate of oil and the average residual stresses. They observed that the increasing the flow rate of oil, the lubricant film thickness and the heat transfer coefficient increase, while the friction coefficient decreases.

3.8 FEM in Micromachining

In some case, to predict the temperature in the tool–chip interface, for example, the use of FEM in machining studies is widely recommended. It is more applied in the micromachining studies due to the smaller dimensions that may complicate the observation of events during the metal cutting. However, while the investigation using FEM in the conventional machining is increasing in the last times; the investigation using FEM in the micromachining is still modest. A search in the Engineering Village database using the word “Finite Element” AND “machining OR milling OR turning or drilling” limited to “Subject/Title/Abstract” was presented an average value of 22,089 publications with this matchup. Replacing the “machining OR milling OR turning OR drilling” by “micromachining OR micro-milling OR micro-turning or micro-drilling”, the result was an average of 183 publications, Fig. 3.3.

Although the micromachining processes present many researches employed experimental or numeric test, this theme has already several gaps to fill out. FEM is used in nanoscale cutting simulation to clarify the chip removal of nanoscale cutting and to re-examine the cutting process in general, that is necessary to understanding of physic of micro-cutting to develop and improve the process of ultra-precision metal cutting technology [83].

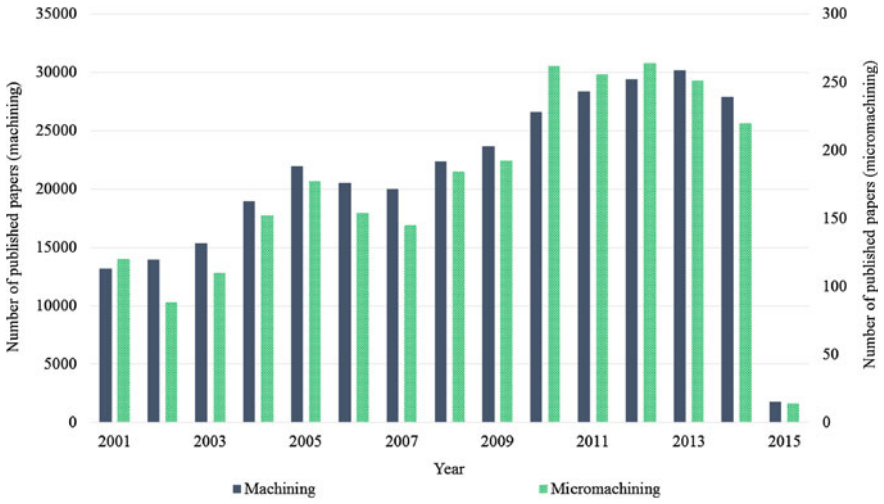

Fig. 3.3 The usage of FEM in conventional and micromachining [82]

Woon et al. [84] cited the first difficulties to simulate micromachining process using FEM, which were technically infeasible due to computing resources required are too intensive becoming this modelling did not too reliable for machining:

- the inabilities of pure Lagrangian solution to manage large element distortions without using unrealistic chip separation criteria, while pure Eulerian solution is impractical for chip formation study as prior assumptions of the chip flow and shape are required to be determined;
- the numerical methods were unable to describe severe plastic deformation in micromachining because accurate solution methods, frictional and material models were not available;
- FEM of micromachining requires large amount of elements at sub-micron to generate an extremely fine mesh to capture insightful transient behaviour of the process.

Maybe because the tool and workpiece size is smaller, some researchers choose to work with FEM. Ding et al. [85] used the FEM to observe in difficult-to-machine materials (Ti-6Al-4V, Inconel 718 and stainless steel AISI 422SS) the application of laser-assisted micro-milling that can eliminate or reduce built-up edge formation.

The micromachining processes are applied to study influence of parameters, events and/or phenomena during or after the cutting. Wang et al. [86] developed a study quantitatively of the chip formation mechanism in micro-milling of Al6061-T6 alloy with a carbide tool using a hybrid FEM analytical approach. They observed that the simulated chip morphology, segment length and cutting force matched the experimental results with acceptable error.

Chen et al. [87] used an energy density-based ductile failure model to study the temperature of tool and workpiece in the micro-cutting of 2A12-T4 aluminium

alloy. The energy density-based ductile failure material model was developed to maintain material deformation behaviour at different mesh distribution in micro-cutting simulation. Furthermore, they observed maximum relative errors between the experimental and simulated temperatures of tool tip and workpiece surface lie between 10 and 20 % under different conditions.

In the laser-assisted micro-milling (LAMM) study, Ding et al. [85] used a 3D finite volume prismatic thermal model to accurately predict the temperature distribution due the laser heating in different LAMM configurations. They also used a 2D finite element models to simulate the continuous chip formation with varying chip thickness in LAMM side cutting with the strain gradient material constitutive models. Among the results, the FE model simulations showed that LAMM could eliminate or reduce the BUE formation in micromachining of difficult-to-machine materials.

To simulate the 2-D micro-milling of Ti-6Al-4V alloy titanium model with feed rate of 4.5 μm/tooth, Özel et al. [88] considered a workpiece with the undeformed chip geometry with a mesh containing 25,000 quadrilateral elements and element size ranging from 0.1 to 3 μm and a micro-tool with a mesh containing 2,500 elements with minimum element size of 0.1 μm.

Huang and Hu [89] cited that the micro-turning process simulation can help observe events that in the experimental during micro-turning are the difficult to observe. They used a 3D model to study the single-grain ceramic influences in the forces, temperature and tool wear.

Maranhão et al. [90] studied the orthogonal cutting of the AISI 1045 with a ISO K10 tool without coating that analyzed the cutting forces, temperature, stresses and displacements. To valid the experimental, they compared the cutting force with experimental results and found an error between 1.89 and 6.18 %. In the temperature analysis, they observed the increase of temperature from 320 to 522 °C with an increase of the feed from 10 to 80 μm/rev. It can be justified as the quantity of energy needed to shear a higher material volume.

Woon et al. [84] used the FEM in micro-milling to investigate the tool edge radius effect, whose the central idea was understand the size differences between the cutting magnitude and tool edge radius rather than emphasizing solely on either one of the parameters separately. In the study of performance of uncoated and cBN coated micro-tools, Özel et al. [88] used the FEM to predict the temperatures and wear development in micromachining of Ti-6Al-4V titanium alloy.

3.8.1 MaterialModelling

The usage of FEM in machining requires much attention. The application the Johnson–Cook (JC) and Coulomb's friction models present good results [86]. However, the material can be of the same order as the grain size and cannot be treated as isotropic and homogeneous, moreover, the FE modelling of micromachining has to be taken into account the size effect [91].

Abouridouane et al. [92] used a 3D thermo-mechanically model to understand the size effects occurring in micro-drilling of AISI 1045 carbon steel. The material modelling was constituted by two-phase (ferrite-pearlite). They affirmed that the cutting process in the micro scale is very complicated and the most model developed considering the heterogeneous materials are still limited currently to two-dimensional orthogonal cut and only give a qualitative prediction of simple plane strain cutting processes.

Bajpai and Singh [93] developed a model of orthogonal machining of Pyrolytic Carbon (PyC) that was constituted by layered anisotropic material presenting errors in the prediction of cutting/thrust forces lie between 9 and 27 %. The damage model used in this paper considered the material response below the elastic limit as well as the post-failure response beyond cracking strain in the strain softening regime in tension.

Zahedi et al. [94] developed a smoothed Particle Hydrodynamic (SPH) approach, which is known as an efficient and numerically robust way for solving large-deformation problems, in modelling micro-turning of single-crystal copper. In this paper, the authors calculated the influence of the anisotropic crystallographic orientations on cutting energy. The variation of cutting energy with different crystallographic orientations can vary up to 400 % for micromachining process of crystalline copper.

According to Zahedi et al. [95], the importance of grain orientation and direction of micromachining on the overall cutting forces, chip morphology was demonstrated together with propensity of the workpiece materialto generate slips when its grains undergo rotations. They observed that total difference in force for the chosen orientations was 33 %, signifying the strength of the effect of crystal orientation in micromachining process.

To study the micro-milling of AISI H13 with different hardness, Afazov et al. [96] applied the proposed method by Yan et al. [45]. They implemented into software a subroutine that needs to be defined for each integration/material point of the FE model. They observed that this methodology had been successfully developed to predict the relationship between cutting forces, uncut chip thickness and cutting velocity with material with different hardness.

3.8.2 Friction

An aspect that requires great attention is the friction coefficient that generally in the macromachining; the friction coefficient is around of 0.5. However, in the micromachining literature is possible to find a high range of friction coefficient. The Table 3.4 exhibits some values found in the literature.

Özel et al. [88] assigned on the micro-milling of Ti-6Al-4V alloy titanium with speed cutting of 75 m/min and a feed per tooth of 4.5 μm/tooth a sliding friction contact (μ) of 0.7 for WC/Co and 0.4 for cBN coating. They perceived that the lowest temperature rise in the cBN coated WC/Co tool due to a lower friction coefficient and higher effective thermal conductivity.

Table 3.4 Friction coefficient applied in micromachining

Researcher	Process	Material	Friction
Woon et al. [84]	Orthogonal cutting	AISI 4340 steel (HR_C 33)	0.1
Abouridouane et al. [92]	Drilling	AISI 1045	0.2
Moriwaki et al. [97]	Orthogonal cutting	Copper	0.7
Wang et al. [86]	Milling	Al 6061-T6 Aluminium alloy	0.7
Ding et al. [85]	Milling	Ti6Al4 V, Inconel 718, AISI 422	0.65

3.9 Remarks

The FEM can be considered a fundamental tool to develop product, mainly to define manufacturing conditions. To employ the FEM to study the machining processes can help to explain several issue through the important information about the cutting, as temperature, residual stress, force and others. Thus, although the simulation tests consume more time than experimental tests, the FEM can be considered an excellent tool to study machining processes because these tests are more inexpensive and provide more information than experimental tests.

However, the users should take care with the input and output in their tests. They should define warily the attributes, mainly the friction and the material modelling, to obtain reliable results. They also should be borne in mind that the FEM provides approximate results and the experimental results, "reals" values, can vary due to not assigned variables, as the variation of the cutting tool geometry, material porosity, variation of the material structure and others. Ashtakhov [98] affirmed that the advanced numerical methods, as FEM, are no more than a powerful tool that requires very skilful hands to handle and the computer's apparent precision causes an unwarranted confidence in the validity of the resulting numbers. The author also highlighted that the software incorporates many not observed assumptions by the users that influence the validity of the results. This fact requires vigilance and the same visual knowledge and intuitive sense of fitness to obtain a successful computer-aided modelling.

Thus, despite computational advances and the software more friendly, FEM can be considered an excellent tool, but just another tool, to study machining processes and other engineering processes. This paper endorses the use of FEM in machining processes researches; nevertheless, it suggests that the users be wary with their results. To search similar experimental researches and confront the results, even the unwanted, can help the users have a perception of phenomenon that would improve her models.

Acknowledgments The authors would like to thank the Ministry of Education's Coordination for the Improvement of Higher Education Personnel (CAPES). The author C.H. Lauro would like to thank Elsevier and Springer for granting permission for reuse of the published materials.

References

1. Liu PF, Zheng JY (2008) Progressive failure analysis of carbon fiber/epoxy composite laminates using continuum damage mechanics. Mater Sci Eng A 485:711–717. doi:10.1016/j.msea.2008.02.023
2. Silva TAA, Panzera TH, Brandão LC et al (2012) Preliminary investigations on auxetic structures based on recycled rubber. Phys Status Solidi 249:1353–1358. doi:10.1002/pssb.201084225
3. Özel T, Altan T (2000) Process simulation using finite element method—prediction of cutting forces, tool stresses and temperatures in high-speed flat end milling. Int J Mach Tools Manuf 40:713–738. doi:10.1016/S0890-6955(99)00080-2
4. Fish J, Belytschko T (2007) A first course in finite elements. doi:10.1002/9780470510858
5. Shaw MC (2004) Metal cutting principles, 2nd edn. Oxford University Press, New York
6. Childs THC, Maekawa K, Obikawa T, Yamane Y (2000) Metal machining theory and applications. Arnold, London
7. Astakhov VP, Outeiro JC (2008) Metal cutting mechanics finite element modelling. In: Davim JP (ed) Machining. Fundamentals and recent advances, 1st edn. Springer, London, pp 13–25
8. Arrazola PJ, Özel T, Umbrello D et al (2013) Recent advances in modelling of metal machining processes. CIRP Ann Manuf Technol 62:695–718. doi:10.1016/j.cirp.2013.05.006
9. Fallböhmer P, Rodríguez CA, Özel T, Altan T (2000) High-speed machining of cast iron and alloy steels for die and mold manufacturing. J Mater Process Technol 98:104–115. doi:10.1016/S0924-0136(99)00311-8
10. Elbestawi MA, Chen L, Becze CE, El-Wardany TI (1997) High-speed milling of dies and molds in their hardened state. CIRP Ann Manuf Technol 46:57–62. doi:10.1016/S0007-8506(07)60775-6
11. Stenberg N, Proudian J (2013) Numerical modelling of turning to find residual stresses. In: Procedia CIRP 14th CIRP conference model machining operations, vol 8, pp 258–264. doi:10.1016/j.procir.2013.06.099
12. Gardner JD, Vijayaraghavan A, Dornfeld DA (2005) Comparative study of finite element simulation software. In: Lab Manuf Autom http://escholarship.org/uc/item/8cw4n2tf. Accessed 19 Nov 2013
13. Amini S, Soleimanimehr H, Nategh MJ et al (2008) FEM analysis of ultrasonic-vibration-assisted turning and the vibratory tool. J Mater Process Technol 201:43–47. doi:10.1016/j.jmatprotec.2007.11.271
14. Zanger F, Schulze V (2013) Investigations on mechanisms of tool wear in machining of Ti-6Al-4V using FEM simulation. In: Procedia CIRP 14th CIRP conference on modeling of machining operations, vol 8, pp 158–163. doi:10.1016/j.procir.2013.06.082
15. Dandekar CR, Shin YC, Barnes J (2010) Machinability improvement of titanium alloy (Ti-6Al-4V) via LAM and hybrid machining. Int J Mach Tools Manuf 50:174–182. doi:10.1016/j.ijmachtools.2009.10.013
16. Muhammad R, Ahmed N, Roy A, Silberschmidt VV (2012) Numerical modelling of vibration-assisted turning of Ti-15333. Procedia CIRP 1:347–352. doi:10.1016/j.procir.2012.04.062
17. Maranhão C, Davim JP (2010) Finite element modelling of machining of AISI 316 steel: numerical simulation and experimental validation. Simul Model Pract Theory 18:139–156. doi:10.1016/j.simpat.2009.10.001
18. John MRS, Shrivastava K, Banerjee N et al (2013) Finite element method-based machining simulation for analyzing surface roughness during turning operation with HSS and carbide insert tool. Arab J Sci Eng 38:1615–1623. doi:10.1007/s13369-013-0541-1
19. Lauro CH, Brandão LC, Januário T et al (2013) An approach to define the heat flow in drilling with different cooling systems using finite element analysis. Adv Mech Eng 2013:9. doi:10.1155/2013/612747

20. Isbilir O, Ghassemieh E (2011) Finite element analysis of drilling of titanium alloy. In: Procedia engineering—11th international conference on the mechanical behavior of materials, vol 10, pp 1877–1882. doi:10.1016/j.proeng.2011.04.312
21. Schulze V, Osterried J, Strauß T (2011) FE analysis on the influence of sequential cuts on component conditions for different machining strategies. Procedia Eng 19:318–323. doi:10.1016/j.proeng.2011.11.119
22. Davim JP, Maranhão C, Jackson MJ et al (2007) FEM analysis in high speed machining of aluminium alloy (Al7075-0) using polycrystalline diamond (PCD) and cemented carbide (K10) cutting tools. Int J Adv Manuf Technol 39:1093–1100. doi:10.1007/s00170-007-1299-y
23. Sartkulvanich P, Altan T, Göcmen A (2005) Effects of flow stress and friction models in finite element simulation of orthogonal cutting—a sensitivity analysis. Mach Sci Technol 9:1–26. doi:10.1081/MST-200051211
24. Ali MH, Ansari MNM, Khidhir BA et al (2014) Simulation machining of titanium alloy (Ti-6Al-4V) based on the finite element modeling. J Brazilian Soc Mech Sci Eng 36:315–324. doi:10.1007/s40430-013-0084-0
25. Rizzuti S, Umbrello D, Filice L, Settineri L (2010) Finite element analysis of residual stresses in machining. Int J Mater Form 3:431–434. doi:10.1007/s12289-010-0799-
26. Doman D, Warkentin A, Bauer R (2009) Finite element modeling approaches in grinding. Int J Mach Tools Manuf 49:109–116. doi:10.1016/j.ijmachtools.2008.10.002
27. Özel T, Zeren E (2007) Finite element modeling the influence of edge roundness on the stress and temperature fields induced by high-speed machining. Int J Adv Manuf Technol 35:255–267. doi:10.1007/s00170-006-0720-2
28. Benson DJ, Okazawa S (2004) Contact in a multi-material Eulerian finite element formulation. Comput Methods Appl Mech Eng 193:4277–4298. doi:10.1016/j.cma.2003.12.061
29. Carroll JT, Strenkowski JS (1988) Finite element models of orthogonal cutting with application to single point diamond turning. Int J Mech Sci 30:899–920. doi:10.1016/0020-7403(88)90073-2
30. Nasr MNA, Ng E-G, Elbestawi MA (2008) A modified time-efficient FE approach for predicting machining-induced residual stresses. Finite Elem Anal Des 44:149–161. doi:10.1016/j.finel.2007.11.005
31. Bäker M, Rösler J, Siemers C (2002) A finite element model of high speed metal cutting with adiabatic shearing. Comput Struct 80:495–513. doi:10.1016/S0045-7949(02)00023-8
32. Mamalis AG, Branis AS, Manolakos DE (2002) Modelling of precision hard cutting using implicit finite element methods. J Mater Process Technol 123:464–475. doi:10.1016/S0924-0136(02)00133-4
33. Coelho RT, Ng E, Elbestawi MA (2007) Tool wear when turning hardened AISI 4340 with coated PcBN tools using finishing cutting conditions. Int J Mach Tools Manuf 47:263–272. doi:10.1016/j.ijmachtools.2006.03.020
34. Hu F, Li D (2011) Modelling and simulation of milling forces using an arbitrary Lagrangian-Eulerian finite element method and support vector regression. J Optim Theory Appl 153:461–484. doi:10.1007/s10957-011-9927-y
35. Simoneau A, Ng E, Elbestawi MA (2006) Chip formation during microscale cutting of a medium carbon steel. Int J Mach Tools Manuf 46:467–481. doi:10.1016/j.ijmachtools.2005.07.019
36. Buchkremer S, Wu B, Lung D et al (2013) FE-simulation of machining processes with a new material model. J Mater Process Technol. doi:10.1016/j.jmatprotec.2013.10.014
37. Johnson GR, Cook WH (1985) Fracture characteristics of three metals subjected to various strains, strain rates, temperatures and pressures. Eng Fract Mech 21:31–48. doi:10.1016/0013-7944(85)90052-9
38. Dandekar CR, Shin YC (2012) Modeling of machining of composite materials: a review. Int J Mach Tools Manuf 57:102–121. doi:10.1016/j.ijmachtools.2012.01.006
39. Sartkulvanich P, Koppka F, Altan T (2004) Determination of flow stress for metal cutting simulation—a progress report. J Mater Process Technol 146:61–71. doi:10.1016/S0924-0136(03)00845-8

40. Chen G, Ren C, Yang X et al (2011) Finite element simulation of high-speed machining of titanium alloy (Ti–6Al–4 V) based on ductile failure model. Int J Adv Manuf Technol 56:1027–1038. doi:10.1007/s00170-011-3233-6
41. Ambati R, Yuan H (2010) FEM mesh-dependence in cutting process simulations. Int J Adv Manuf Technol 53:313–323. doi:10.1007/s00170-010-2818-9
42. Duan C, Zhang L (2012) A reliable method for predicting serrated chip formation in high-speed cutting: analysis and experimental verification. Int J Adv Manuf Technol 64:1587–1597. doi:10.1007/s00170-012-4125-0
43. Shrot A, Bäker M (2012) Determination of Johnson-Cook parameters from machining simulations. Comput Mater Sci 52:298–304. doi:10.1016/j.commatsci.2011.07.035
44. Umbrello D, M'Saoubi R, Outeiro JC (2007) The influence of Johnson-Cook material constants on finite element simulation of machining of AISI 316L steel. Int J Mach Tools Manuf 47:462–470. doi:10.1016/j.ijmachtools.2006.06.006
45. Yan H, Hua J, Shivpuri R (2007) Flow stress of AISI H13 die steel in hard machining. Mater Des 28:272–277. doi:10.1016/j.matdes.2005.06.017
46. Becze CE, Worswick MJ, Elbestawi M (2001) High strain rate shear evaluation and characterization of Aisi D2 tool steel in its hardened state. Mach Sci Technol 5:131–149. doi:10.1081/MST-100103182
47. Liu R, Melkote S, Pucha R et al (2013) An enhanced constitutive material model for machining of Ti–6Al–4 V alloy. J Mater Process Technol 213:2238–2246. doi:10.1016/j.jmatprotec.2013.06.015
48. Mocko W, Kowalewski ZL (2013) Perforation test as an accuracy evaluation tool for a constitutive model of austenitic steel. Arch Metall Mater 58:1105–1110. doi:10.2478/amm-2013-0133
49. Zerilli FJ, Armstrong RW (1987) Dislocation-mechanics-based constitutive relations for material dynamics calculations. J Appl Phys 61:1816. doi:10.1063/1.338024
50. Tang L, Huang J, Xie L (2010) Finite element modeling and simulation in dry hard orthogonal cutting AISI D2 tool steel with cBN cutting tool. Int J Adv Manuf Technol 53:1167–1181. doi:10.1007/s00170-010-2901-2
51. Fathipour M, Hamedi M, Yousefi R (2013) Numerical and experimental analysis of machining of Al (20 vol% SiC) composite by the use of ABAQUS software. Materwiss Werksttech 44:14–20. doi:10.1002/mawe.201300959
52. Santiuste C, Soldani X, Miguélez MH (2010) Machining FEM model of long fiber composites for aeronautical components. Compos Struct 92:691–698. doi:10.1016/j.compstruct.2009.09.021
53. Manikandan G, Uthayakumar M, Aravindan S (2012) Machining and simulation studies of bimetallic pistons. Int J Adv Manuf Technol 66:711–720. doi:10.1007/s00170-012-4359-x
54. Seshadri R, Naveen I, Srinivasan S et al (2013) Finite element simulation of the orthogonal machining process with Al 2024 T351 aerospace alloy. Procedia Eng Int Conf Des Manuf 64:1454–1463. doi:10.1016/j.proeng.2013.09.227
55. Kouadri S, Necib K, Atlati S et al (2013) Quantification of the chip segmentation in metal machining: application to machining the aeronautical aluminium alloy AA2024-T351 with cemented carbide tools WC-Co. Int J Mach Tools Manuf 64:102–113. doi:10.1016/j.ijmachtools.2012.08.006
56. Ribeiro Filho SLM, Gomes MO, Lauro CH, Brandão LC (2014) Definition of the temperature and heat flux in micromilling of hardened steel using the finite element method. Arab J Sci Eng 39:7229–7239. doi:10.1007/s13369-014-1281-6
57. Vaz M, Owen DRJ, Kalhori V et al (2007) Modelling and simulation of machining processes. Arch Comput Methods Eng 14:173–204. doi:10.1007/s11831-007-9005-7

58. Schulze V, Zanger F, Boev N (2013) Numerical investigations on changes of the main shear plane while broaching. Procedia CIRP 8:246–251. doi:10.1016/j.procir.2013.06.097
59. Saffar RJ, Razfar MR, Zarei O, Ghassemieh E (2008) Simulation of three-dimension cutting force and tool deflection in the end milling operation based on finite element method. Simul Model Pract Theory 16:1677–1688. doi:10.1016/j.simpat.2008.08.010
60. Malakizadi A, Sadik I, Nyborg L (2013) Wear mechanism of cBN inserts during machining of bimetal aluminum-grey cast iron engine block. In: 14th CIRP conference on modeling of machining operations, vol 8, pp 188–193. doi:10.1016/j.procir.2013.06.087
61. Pu Z, Umbrello D, Dillon OW et al (2014) Finite element modeling of microstructural changes in dry and cryogenic machining of AZ31B magnesium alloy. J Manuf Process 16:335–343. doi:10.1016/j.jmapro.2014.02.002
62. Arrazola PJ, Özel T (2010) Investigations on the effects of friction modeling in finite element simulation of machining. Int J Mech Sci 52:31–42. doi:10.1016/j.ijmecsci.2009.10.001
63. Özel T (2006) The influence of friction models on finite element simulations of machining. Int J Mach Tools Manuf 46:518–530. doi:10.1016/j.ijmachtools.2005.07.001
64. Haddag B, Atlati S, Nouari M, Znasni M (2010) Finite element formulation effect in three-dimensional modeling of a chip formation during machining. Int J Mater Form 3:527–530. doi:10.1007/s12289-010-0823-z
65. Ulutan D, Özel T (2013) Determination of tool friction in presence of flank wear and stress distribution based validation using finite element simulations in machining of titanium and nickel based alloys. J Mater Process Technol 213:2217–2237. doi:10.1016/j.jmatprotec.2013.05.019
66. Özel T, Altan T (2000) Determination of workpiece flow stress and friction at the chip–tool contact for high-speed cutting. Int J Mach Tools Manuf 40:133–152. doi:10.1016/S0890-6955(99)00051-6
67. Özel T (2009) Computational modelling of 3D turning: influence of edge micro-geometry on forces, stresses, friction and tool wear in PcBN tooling. J Mater Process Technol 209:5167–5177. doi:10.1016/j.jmatprotec.2009.03.002
68. Rotella G, Dillon OW, Umbrello D et al (2013) Finite element modeling of microstructural changes in turning of AA7075-T651 alloy. J Manuf Process 15:87–95. doi:10.1016/j.jmapro.2012.09.005
69. Klinkova O, Rech J, Drapier S, Bergheau J-M (2011) Characterization of friction properties at the workmaterial/cutting tool interface during the machining of randomly structured carbon fibers reinforced polymer with carbide tools under dry conditions. Tribol Int 44:2050–2058. doi:10.1016/j.triboint.2011.09.006
70. Mahdi M, Zhang L (2001) A finite element model for the orthogonal cutting of fiber-reinforced composite materials. J Mater Process Technol 113:373–377. doi:10.1016/S0924-0136(01)00675-6
71. Phadnis VA, Roy A, Silberschmidt VV (2013) A finite element model of ultrasonically assisted drilling in carbon/epoxy composites. Procedia CIRP 8:141–146. doi:10.1016/j.procir.2013.06.079
72. Phadnis VA, Roy A, Silberschmidt VV (2012) Finite element analysis of drilling in carbon fiber reinforced polymer composites. J Phys: Conf Ser 382:012014. doi:10.1088/1742-6596/382/1/012014
73. Pramanik A, Zhang LC, Arsecularatne JA (2007) An FEM investigation into the behavior of metal matrix composites: Tool–particle interaction during orthogonal cutting. Int J Mach Tools Manuf 47:1497–1506. doi:10.1016/j.ijmachtools.2006.12.004
74. Childs THC (2013) Ductile shear failure damage modelling and predicting built-up edge in steel machining. J Mater Process Technol 213:1954–1969. doi:10.1016/j.jmatprotec.2013.05.017
75. Weinert K, Schneider M (2000) Simulation of tool-grinding with finite element method. CIRP Ann Manuf Technol 49:253–256. doi:10.1016/S0007-8506(07)62940-0

76. Duan C, Kong W, Hao Q, Zhou F (2013) Modeling of white layer thickness in high speed machining of hardened steel based on phase transformation mechanism. Int J Adv Manuf Technol 69:59–70. doi:10.1007/s00170-013-5005-y
77. Attanasio A, Umbrello D, Cappellini C et al (2012) Tool wear effects on white and dark layer formation in hard turning of AISI 52100 steel. Wear 286–287:98–107. doi:10.1016/j.wear.2011.07.001
78. Ramesh A, Melkote SN (2008) Modeling of white layer formation under thermally dominant conditions in orthogonal machining of hardened AISI 52100 steel. Int J Mach Tools Manuf 48:402–414. doi:10.1016/j.ijmachtools.2007.09.007
79. Ee KC, Dillon OW, Jawahir IS (2005) Finite element modeling of residual stresses in machining induced by cutting using a tool with finite edge radius. Int J Mech Sci 47:1611–1628. doi:10.1016/j.ijmecsci.2005.06.001
80. Valiorgue F, Rech J, Hamdi H et al (2012) 3D modeling of residual stresses induced in finish turning of an AISI304L stainless steel. Int J Mach Tools Manuf 53:77–90. doi:10.1016/j.ijmachtools.2011.09.011
81. Ji X, Zhang X, Liang SY (2013) Predictive modeling of residual stress in minimum quantity lubrication machining. Int J Adv Manuf Technol. doi:10.1007/s00170-013-5439-2
82. Engineering Village (2015) Number of published papers about finite element method in machining process. www.engineeringvillage.com
83. Mackerle J (1999) Finite-element analysis and simulation of machining: a bibliography (1976–1996). J Mater Process Technol 86:17–44. doi:10.1016/S0924-0136(98)00227-1
84. Woon KS, Rahman M, Fang FZ et al (2008) Investigations of tool edge radius effect in micromachining: a FEM simulation approach. J Mater Process Technol 195:204–211. doi:10.1016/j.jmatprotec.2007.04.137
85. Ding H, Shen N, Shin YC (2012) Thermal and mechanical modeling analysis of laser-assisted micro-milling of difficult-to-machine alloys. J Mater Process Technol 212:601–613. doi:10.1016/j.jmatprotec.2011.07.016
86. Wang J, Gong Y, Abba G et al (2009) Chip formation analysis in micromilling operation. Int J Adv Manuf Technol 45:430–447. doi:10.1007/s00170-009-1989-8
87. Chen G, Ren C, Zhang P et al (2013) Measurement and finite element simulation of micro-cutting temperatures of tool tip and workpiece. Int J Mach Tools Manuf 75:16–26. doi:10.1016/j.ijmachtools.2013.08.005
88. Özel T, Thepsonthi T, Ulutan D, Kaftanoğlu B (2011) Experiments and finite element simulations on micro-milling of Ti–6Al–4 V alloy with uncoated and cBN coated micro-tools. CIRP Ann Manuf Technol 60:85–88. doi:10.1016/j.cirp.2011.03.087
89. Huang W-J, Hu H-J (2014) Micro-turning of hard steel by single-grain ceramic cutter based on numerical simulations. Ceram Int. doi:10.1016/j.ceramint.2014.05.002
90. Maranhão C, da Silva LR, Davim JP (2013) Comportamento termo mecânico no micro-torneamento ortogonal do aço AISI 1045 (Ck45 - DIN): Simulação via elementos finitos e validação experimental. Ciência Tecnol dos Mater 25:57–66. doi:10.1016/j.ctmat.2013.12.006
91. Klocke F, Gerschwiler K, Abouridouane M (2009) Size effects of micro drilling in steel. Prod Eng 3:69–72. doi:10.1007/s11740-008-0144-y
92. Abouridouane M, Klocke F, Lung D, Adams O (2012) Size effects in micro drilling ferritic-pearlitic carbon steels. 45th CIRP Conf. Manuf Syst 3:91–96. doi:10.1016/j.procir.2012.07.017
93. Bajpai V, Singh RK (2014) Finite element modeling of orthogonal micromachining of anisotropic pyrolytic carbon via damaged plasticity. Precis Eng 38:300–310. doi:10.1016/j.precisioneng.2013.10.004
94. Zahedi SA, Roy A, Silberschmidt VV (2013) Modeling of micro-machining single-crystal f.c.c. metals. Procedia CIRP 8:346–350. doi:10.1016/j.procir.2013.06.114
95. Zahedi SA, Demiral M, Roy A, Silberschmidt VV (2013) FE/SPH modelling of orthogonal micro-machining of f.c.c. single crystal. Comput Mater Sci 78:104–109. doi:10.1016/j.commatsci.2013.05.022

96. Afazov SM, Ratchev SM, Segal J (2011) Prediction and experimental validation of micro-milling cutting forces of AISI H13 steel at hardness between 35 and 60 HR_C. Int J Adv Manuf Technol 62:887–899. doi:10.1007/s00170-011-3864-7
97. Moriwaki T, Sugimura N, Luan S (1993) Combined stress, material flow and heat analysis of orthogonal micromachining of copper. CIRP Ann Manuf Technol 42:75–78. doi:10.1016/S0007-8506(07)62395-6
98. Ashtakhov VP (2002) Metal cutting theory—missed chances or a science without history: Part 2. In: Pers. Vis. Viktor P. Astakhov. http://viktorastakhov.tripod.com/mc2.pdf. Accessed 1 Jan 2015